42. Kumar G, Waters MS, Farooque TM, Young MF, Simon CG Jr. Freeform fabricated scaffolds with roughened struts that enhance both stem cell proliferation and differentiation by controlling cell shape. Biomaterials 2012;33:4022–4030.
43. Simon AM, Manigrasso MB, O'Connor JP. Cyclo-oxygenase 2 function is essential for bone fracture healing. J Bone Miner Res 2002;17:963–976.
44. Lee HW, Kim SY, Kim AY, Lee EJ, Choi J-Y, Kim JB. Adiponection stimulates osteoblast differntiation through induction of COX2 in mesenchymal progenitor cells. Stem Cells 2009;27: 2254–2262.
45. Chikazu D, Li X, Kawaguchi H, Sakuma Y, Voznesensky OS, Adams DJ, Xu M, Hoshi K, Katavic V, Herschman HR, Raisz L, Pilbeam CC. Bone morphogenetic protein 2 induces cyclo-oxygenase 2 in osteoblasts via Cbfa1 binding site: Role in effects of bone mprphogenetic protein 2 in vitro and in vivo. J Bone Miner Res 2002;17:1430–1440.
46. Susperregui ARG, Gamell C, Rodíguez-Carballo E, Ortuño MJ, Bartrons R, Rosa JL, Ventura F. Noncanonical BMP signaling regulates *Cyclooxygenase-2* transcription. Mol Endocrinol 2011;25: 1006–1017.
47. Peiris D, Pacheco I, Spencer C, MacLeod RJ. The extracellular calcium-sensing receptor reciprocally regulates the secretion of BMP-2 and the BMP antagonist Noggin in colonic myofibroblasts. Am J Physiol Gastrointest Liver Physiol 2007;292:G753–G766.
48. Tada H, Nemoto E, Kanaya S, Hamaji N, Sato H, Shimauchi H. Elevated extracellular calcium increases expression of bone morphogenetic protein-2 gene via a calcium channel and ERK pathway in human dental pulp cells. Biochem Biophys Res Commun 2010;394:1093–1097.
49. Huang H, Chikazu D, Voznesensky OS, Herschman HR, Kream BE, Drissi H, Pilbeam CC. Parathyroid hormone induction of cycloxygenase-2 in murine osteoblasts: Role of the calcium–calcineurin–NFAT pathway. J Bone Miner Res 2010;25:819–829.
50. Day TF, Guo X, Garrett-Beal L, Yang Y. Wnt/beta-catenin signaling in mesenchymal progenitors controls osteoblast and chondrocyte differentiation during vertebrate skeletogenesis. Dev Cell 2005;8: 739–750.
51. Olivares-Navarrete R, Hyzy SL, Park JH, Dunn GR, Haithcock DA, Wasilewski CE, Boyan BD, Schwartz Z. Mediation of osteogenic differentiation of human mesenchymal stem cells on titanium surfaces by a Wnt-integrin feedback loop. Biomaterials 2011;32:6399–6411.

Langmuir

Article

pubs.acs.org/Langmuir

Quantitative Evaluation of Interaction Force between Functional Groups in Protein and Polymer Brush Surfaces

Sho Sakata,[†] Yuuki Inoue,*[,†] and Kazuhiko Ishihara*[,†,‡]

[†]Department of Materials Engineering, [‡]Department of Bioengineering, School of Engineering, The University of Tokyo, 7-3-1, Hongo, Bunkyo-ku, Tokyo 113-8656, Japan

Supporting Information

ABSTRACT: To understand interactions between polymer surfaces and different functional groups in proteins, interaction forces were quantitatively evaluated by force-versus-distance curve measurements using atomic force microscopy with a functional-group-functionalized cantilever. Various polymer brush surfaces were systematically prepared by surface-initiated atom transfer radical polymerization as well-defined model surfaces to understand protein adsorption behavior. The polymer brush layers consisted of phosphorylcholine groups (zwitterionic/hydrophilic), trimethylammonium groups (cationic/hydrophilic), sulfonate groups (anionic/hydrophilic), hydroxyl groups (nonionic/hydrophilic), and *n*-butyl groups (nonionic/hydrophobic) in their side chains.

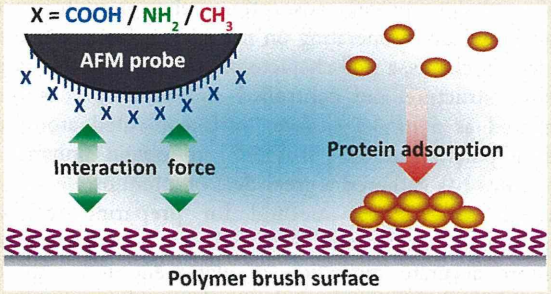

The interaction forces between these polymer brush surfaces and different functional groups (carboxyl groups, amino groups, and methyl groups, which are typical functional groups existing in proteins) were quantitatively evaluated by force-versus-distance curve measurements using atomic force microscopy with a functional-group-functionalized cantilever. Furthermore, the amount of adsorbed protein on the polymer brush surfaces was quantified by surface plasmon resonance using albumin with a negative net charge and lysozyme with a positive net charge under physiological conditions. The amount of proteins adsorbed on the polymer brush surfaces corresponded to the interaction forces generated between the functional groups on the cantilever and the polymer brush surfaces. The weakest interaction force and least amount of protein adsorbed were observed in the case of the polymer brush surface with phosphorylcholine groups in the side chain. On the other hand, positive and negative surfaces generated strong forces against the oppositely charged functional groups. In addition, they showed significant adsorption with albumin and lysozyme, respectively. These results indicated that the interaction force at the functional group level might be a suitable parameter for understanding protein adsorption.

1. INTRODUCTION

Protein adsorption on the material surfaces is well-known as an initial and important event that determines subsequent biological responses.[1,2] In particular, unfavorable protein adsorption on the surface of biomedical devices may cause several serious biological problems (for example, thrombus formation, immunoreactions, and inflammatory response). Moreover, the performance of biomedical devices decreases significantly because of the protein adsorption layer on the devices. Therefore, protein adsorption behavior should be precisely understood and carefully considered during the development of biomedical devices that are to be used in biological environments for long periods. During the last 40 years, many studies have been carried out to understand protein adsorption behavior on surfaces: however, the process still remains considerably unclear. Protein adsorption occurs in a very complex way through the various intermolecular and surface forces generated between material surfaces and proteins. Interactions are induced by van der Waals forces, electrostatic interactions, hydrophobic interactions, and hydrogen bonding.[3] By measuring and evaluating these forces, we will be able to gain a better understanding of protein adsorption on a material surface.

Recently, force measurement methodology using atomic force microscopy (AFM) has developed as a powerful tool to directly measure the interaction force between two surfaces in the range of a few nanonewtons.[4−14] In biomedical research fields, the quantification of the direct interaction force between biomolecules immobilized on surfaces and AFM probes, such as antigen−antibody and ligand−receptor, has been accomplished.[5−8] The direct molecular interaction force between proteins and material surfaces has also been evaluated for self-assembled monolayers, polymer-grafted surfaces, and dense polymer brush surfaces.[9−14] These interaction forces are considered to originate from interactions between various functional groups existing in proteins and those exposed on material surfaces. Proteins are polypeptides composed of various amino acid residues having specific functional groups in the side chain. In general, hydrophilic functional groups are

Received: December 28, 2013
Revised: February 12, 2014

   dx.doi.org/10.1021/la404981k | *Langmuir* XXXX, XXX, XXX−XXX

natively exposed on the surface of proteins in aqueous media. However, with protein adsorption onto material surfaces, the conformation of the adsorbed proteins changes because of the direct interaction with the surface, which leads to irreversible adsorption. These phenomena have been theoretically explained by Lu et al.[15] Therefore, a quantitative analysis of the interaction force at the functional group level on the surfaces would provide the basis for understanding protein adsorption. Carboxyl groups, amino groups, and methyl groups are the representative functional groups that are present in the amino acid residues of proteins and are anionic (hydrophilic), cationic (hydrophilic), and hydrophobic in nature, respectively. Therefore, the interaction forces using these functional groups will mainly give an indication of electrostatic and hydrophobic interactions.

To consider protein adsorption behavior in terms of the interaction forces operating on material surfaces at the level of molecular chains, a well-characterized surface possessing precise surface structure and controlled surface properties must be prepared as a model surface. Surface-initiated atom transfer radical polymerization (SI-ATRP) to obtain polymer brush structures has gathered a great deal of attention because it is a versatile and robust method for preparing well-defined structures on a substrate.[16,17] A polymer brush surface enables a more accurate regulation of alignment and state of the molecular chains, compared to the surfaces prepared by conventional methods such as polymer-coating. In addition, its physicochemical surface properties such as surface free energy and surface potential can be controlled easily by the chemical structure of the monomer unit and its three-dimensional structure. It is well-known that the amount of protein adsorbed on a surface is suppressed significantly in some types of polymer brush surfaces.[18−25] This demonstrates the importance of a model surface for the accurate understanding of the relationship between protein adsorption behavior and interaction forces. Furthermore, analyses on systematically constructed polymer brush surfaces will lead to new design concepts for novel biointerfaces that suppress protein adsorption effectively.

2. EXPERIMENTAL SECTION

2.1. Materials. 2-Methacryloyloxyethyl phosphorylcholine (MPC) was purchased from NOF Corp. (Tokyo, Japan), which was synthesized and purified according to a previously reported method.[26] 2-Trimethylammoniumethyl methacrylate chloride (TMAEMA) and potassium 3-methacryloyloxypropyl sulfonate (SPMA) were purchased from Tokyo Chemical Industry Company, Ltd. (Tokyo, Japan) and used as received. Ethyl-2-bromoisobutyrate (EBIB), 4,4′-dinonyl-2,2′-bipyridyl (DNbpy), and 2-hydroxyethyl methacrylate (HEMA) were purchased from Sigma-Aldrich Company (St. Louis, MO) and used as received. *n*-Butyl methacrylate (BMA) was purchased from Kanto Chemical Company, Inc. (Tokyo, Japan) and used as received. Copper(I) bromide (CuBr) and 2,2′-bipyridyl (bpy) were purchased from Wako Pure Chemical Industries Ltd. (Osaka, Japan) and used as received. Albumin from bovine serum (Alb) and lysozyme from chicken egg white (Lys) were purchased from Sigma-Aldrich Company (St. Louis, MO) and used as received. All other reagents and solvents of extra-pure grade were commercially available and were used as purchased. Silicon wafers were purchased from Furuuchi Chemical Corp. (Tokyo, Japan); their surfaces were coated with ∼10-nm-thick SiO_2 layers. High-purity grade oxygen and argon gases were used.

2.2. Preparation of Polymer Brush Surfaces. Polymer brush surfaces were prepared on the initiator-immobilized substrates by SI-ATRP, using one of the monomers from MPC, TMAEMA, SPMA, HEMA, and BMA, according to a previously reported procedure (Figure 1).[27] Briefly, a surface-immobilizing initiator [10-(2-bromo-2-methyl)propionyloxy]decyltrichlorosilane (BrC10TCS) was synthesized and immobilized on the silicon wafers, as previously described.[28] CuBr, bpy, and the monomer in a particular molar ratio were dissolved in the degassed solvents in a glass tube. The following solvents were used: methanol for MPC and HEMA at monomer concentrations of 1.0 mol/L, a mixture of methanol and water (70:30 by volume) for TMAEMA at a monomer concentration of 1.0 mol/L, a mixture of methanol and water (50:50 by volume) for SPMA at a monomer concentration of 0.50 mol/L, and a mixture of methanol and 1,4-dioxane (20:80 by volume) for BMA at a monomer concentration of 2.0 mol/L. Potassium chloride of the same concentration as SPMA (0.50 mol/L) was added to the SPMA solution to enhance the solubility of SPMA in an aqueous medium. DNbpy was used as the ligand instead of bpy in the case of polymerization of BMA. Argon was bubbled into the monomer solution at room temperature for 10 min. The BrC10TCS-immobilized substrate was then immersed into the solution, and EBIB was simultaneously added as the free initiator at a defined concentration. After the glass tube was sealed, polymerization was performed at room temperature with stirring. After 24 h, the substrate was removed from the polymerization solution, rinsed with appropriate solvents for each polymer, methanol for poly(MPC), poly(TMAEMA), and poly(HEMA); water for poly(SPMA); and acetone for poly(BMA), and then dried in a nitrogen stream. The expected degree of polymerization (DP, [monomer]/[initiator] ratio in feed) was set at 25, 50, 100, and 200.

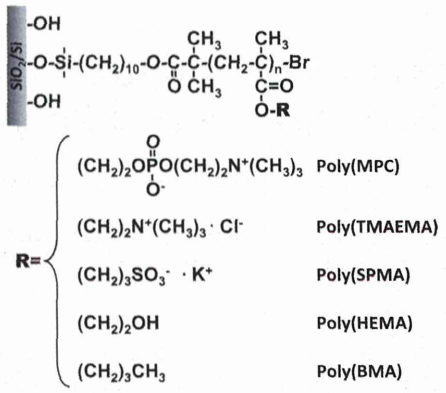

Figure 1. Chemical structure of polymer brush layers.

The conversion of monomer to polymer was determined by proton nuclear magnetic resonance spectroscopy (^{1}H NMR) (*α*-300; JEOL, Tokyo, Japan). The following deuterated solvents were used: methanol-d_4 for poly(MPC), poly(TMAEMA), and poly(HEMA); deuterium oxide for poly(SPMA); and chloroform-d for poly(BMA).

2.3. Surface Characterization. The composition of surface elements was determined using X-ray photoelectron spectroscopy (XPS) (AXIS-His; Shimadzu Company, Kyoto, Japan) with a magnesium anode nonmonochromatic source. The samples were completely dried in vacuo before the measurement. High-resolution scans for C_{1s}, N_{1s}, P_{2p}, S_{2p}, and Br_{3d} were acquired at a takeoff angle of 90° for the photoelectrons. The binding energies were referred to the C_{1s} peak at 285.0 eV. The XPS spectra of polymer brush surfaces are shown in Figure S1 of the Supporting Information.

The surface morphologies of the polymer brush surfaces under dry conditions were observed with an AFM (Nanoscope IIIa; Bruker AXS K.K., Kanagawa, Japan) operated in tapping mode. The measurements were performed using a commercially available cantilever (RTESP with a reported spring constant of 20−80 N/m, Bruker AXS K.K.) at a scan rate of 1.0 Hz with a scan size of 1.0 × 1.0 μm. The root-mean-square (RMS) values of the surface roughness were calculated from the roughness profiles. The height images of the polymer brush surfaces are shown in Figure S2 of the Supporting Information.

dx.doi.org/10.1021/la404981k | *Langmuir* XXXX, XXX, XXX−XXX

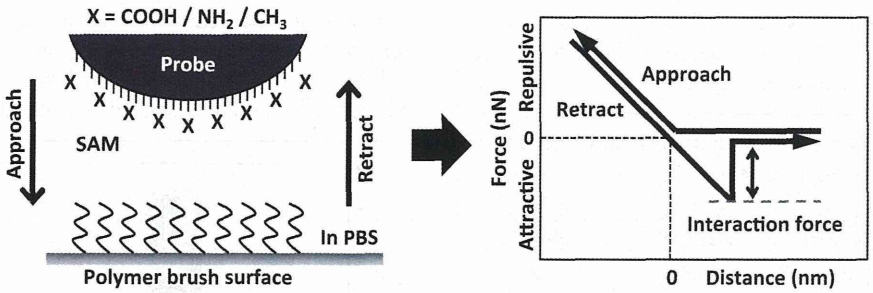

Figure 2. Schematic of the measurement of the interaction force between functional groups and polymer brush surfaces.

The thickness of the polymer brush layers was determined under dry conditions using a spectroscopic ellipsometer (α-SE; J.A. Woolam, Lincoln, NE). The BrC10TCS-immobilized substrate and each polymer brush layer were measured at an incident angle of 70° in the visible region. The thickness of the polymer brush layer was determined using the Cauchy layer model with an assumed refractive index of 1.49 at 632.8 nm. The graft density, σ (chains/nm^2), was calculated from the ellipsometric thickness determined for each polymer brush layer by using the following equation:

$$\sigma = h\rho N_A/M_n$$

where h is the ellipsometric thickness (nm), ρ is the density of each dry polymer [1.30 g/cm^3 for poly(MPC),[18] poly(TMAEMA), and poly(SPMA), and 1.15 g/cm^3 for poly(HEMA)[22] and poly(BMA)], N_A is Avogadro's number, and M_n is the number-average molecular weight of polymer chains on the surface, which was assumed to be the same as the number-average molecular weight of each polymer in the polymerization solution, estimated from the degree of polymerization determined using the ^{1}H NMR spectrum of each free polymer.[29,30]

The static contact angles in an aqueous medium were measured by captive bubble methods using a goniometer (CA-W; Kyowa Interface Science Company Ltd., Saitama, Japan) at room temperature. The samples were immersed in water for 24 h before the measurement. Air bubbles of a 5.0 μL volume were brought in contact with the substrates. All contact angles were directly measured from the photographic images. Data were collected at more than three positions for each sample.

The ζ-potential at the surface was measured by the streaming potential measurement method in a 10 mmol/L sodium chloride solution using a measurement unit (ELS-8000; Otsuka Electronics, Company, Ltd., Osaka, Japan) with an ancillary flat plate cell (10 × 30 × 60 mm) coated with poly(acrylamide) at 25 °C. Polystyrene latex particles (520 nm in diameter, Otsuka Electronics) coated with hydroxypropyl cellulose (M_w = 300 kDa, Scientific Polymer Products, NY) were used as the mobility-monitoring particles. All measurements were repeated at least three times.

2.4. Measurement of the Interaction Force with Functional Groups. The interaction force between the functional groups and the polymer brush surfaces in phosphate-buffered saline (PBS; pH 7.4, ionic strength = 150 mmol/L) was estimated by force-versus-distance (f–d) curve measurements using AFM. A silica bead with a diameter of 20 μm (Duke Scientific Company, Palo Alto, CA) was manually immobilized at the end of a commercial, probeless cantilever (NP-O with reported spring constant of 0.06 N/m, Bruker AXS K.K.), according to a previously reported procedure.[31] Using optical microscopy, we confirmed that the silica bead was successfully immobilized on the cantilever. Then, 3-nm-thick chromium and subsequently 27-nm-thick gold films were sputtered onto the silica-bead-immobilized cantilever. The gold-sputtered cantilever was then immersed in a 1.0 mmol/L solution of 10-carboxy-1-decanethiol, 11-amino-1-undecanethiol, or 1-dodecanethiol in ethanol for 24 h to form a carboxyl group, amino group, or methyl group-terminated self-assembled monolayers (COOH–SAM, NH_2–SAM, or CH_3–SAM) on the silica-bead-immobilized cantilever, respectively.

The interaction force between the self-assembled monolayers on the silica bead-immobilized cantilever and polymer brush layers with target DP of 100 in PBS was evaluated from the approaching and retracting trace of the f–d curve at room temperature, as shown in Figure 2. The shift value of deflection in the retract trace of the f–d curves from the bottom of the retrace line corresponds to the interaction force. In each measurement, more than 100 of the approaching/retracting f–d curves were collected, and the average value was defined as the interaction force between functional groups and substrates. All measurements were performed for at least three polymer brush substrates using the same cantilever.

2.5. Evaluation of Protein Adsorption Mass. The adsorbed amount of proteins on the polymer brush surfaces was quantified with surface plasmon resonance (SPR) (SPR-670M; Moritex Company, Tokyo, Japan).[32] The proteins used in this study were Alb (Isoelectric point: pI = 4.8) and Lys (pI = 11.1).

We prepared the polymer brush layers with the target DP of 100 on SPR gold-chips using the method described above, and 11-(2-bromo-2-methylpropyonyloxy)undecyl mercaptan (BUM) was used as the initiator capable of binding to the thin gold layer on the substrate.[33] The SPR substrates were first exposed to PBS at a flow rate of 500 μL/min, until a stable baseline was established. Thereafter, a 1.0 mg/mL PBS solution of proteins was injected for 30 min, followed by PBS for an additional 10 min to replace protein solution and to wash off the weakly adsorbed proteins from the surface. The change in the resonance angle was used to estimate the amount of adsorbed proteins using the following relationship:[34] Amount of adsorbed proteins (nanogram per squared centimeter) = 500 × increase of resonance angle (degrees). All the measurements were performed at 37 °C and repeated at least three times.

3. RESULTS AND DISCUSSION

3.1. Surface Characterization of Polymer Brush Surfaces. In this study, five kinds of polymer brush layers, poly(MPC), poly(TMAEMA), poly(SPMA), poly(HEMA), and poly(BMA), were prepared on the BrC10TCS-immobilized substrate using SI-ATRP with a free initiator. The surface elements and the surface topology of the polymer brush surfaces were analyzed using XPS and AFM, respectively, according to a previously reported method.[27] We detected the peaks attributed to each monomer unit in the XPS charts (Figure S1 of the Supporting Information). Thus, XPS analysis confirmed the identity of the monomer elements of each polymer chain on the surface of the silicon wafers. The RMS values of the surface roughness analyzed by AFM in dry conditions were comparable to previously reported values, thereby indicating that the polymer brush layers prepared in this study were homogeneous (Figure S2 of the Supporting Information).

The ellipsometric thickness of the polymer brush layers under dry conditions were plotted against the molecular weights of the polymer chains (Figure S3 of the Supporting Information), demonstrating that the thickness of the polymer brush layers could be linearly controlled in the range of 1–25 nm by changing the molecular weight of the grafted polymer

dx.doi.org/10.1021/la404981k | Langmuir XXXX, XXX, XXX–XXX

chains. The calculated graft densities of all polymer chains were greater than 0.10 chains/nm^2, which indicates the formation of highly dense polymer brush structures (Table 1).[16] To characterize the structure of the polymer brush surfaces, the coverage of the polymer brush layers with each polymer chain was evaluated from the value of the graft density and the monomer cross-sectional area, which was calculated from the basic properties of each monomer moiety and the length of the C−C−C bond (i.e., 0.25 nm). The space among the polymer chains calculated from the graft density and the cross-sectional area of the grafted polymer chain for each polymer brush layer was sufficiently narrow compared to the size of proteins used in this study (Alb: 14.0 × 4.0 × 4.0 nm; Lys: 4.5 × 3.0 × 3.0 nm). Therefore, the primary adsorption, in which a protein diffuses into the polymer brush layer and directly adsorbs on the substrate, and the tertiary adsorption, in which a protein interacts with the polymer chains within the polymer brush layer are negligible.[22,35] Model surfaces which simplify the discussion from the aspect of the structure were constructed.

Table 1. Graft Density, Cross-Sectional Area, and Surface Coverage of Polymer Brush Layers

polymer	graft density (chains/nm^2)	cross-sectional area (nm^2)	surface coverage (%)
Poly(MPC)	0.33	1.5	49
Poly(TMAEMA)	0.45	1.1	48
Poly(SPMA)	0.55	1.3	70
Poly(HEMA)	0.66	0.75	49
Poly(BMA)	0.75	0.82	61

We measured the static air bubble contact angles in an aqueous medium at the polymer brush surfaces and plotted them against the ellipsometric thickness of the polymer brush layers (Figure 3). The static air bubble contact angle in aqueous conditions for the BrC10TCS-immobilized silicon substrate was approximately 80°. The static air bubble contact angles for the polymer brush surfaces were lower than that of the BrC10TCS-immobilized substrate, even for thin polymer brush layers, except for the poly(BMA) brush surface, in which the static air bubble contact angle was as high as the BrC10TCS-immobilized substrate. From these results, it can be seen that hydrophilic polymer brush surfaces [except for the poly(BMA) brush surface] in aqueous conditions were prepared, and that hydrophobic interactions would be negligible on these surfaces [except for the poly(BMA) brush surface].

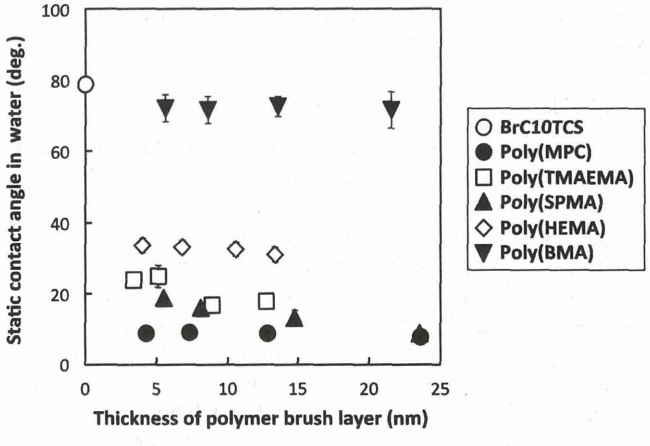

Figure 3. Static contact angles in water of the BrC10TCS-immobilized substrate and polymer brush surfaces.

We measured the ζ-potential of the polymer brush layers in a 10 mmol/L sodium chloride solution (Figure 4). The ζ-potentials of the zwitterionic poly(MPC) brush layer and hydrophilic poly(HEMA) brush layers were almost zero (−5.9 mV and −8.8 mV, respectively). On the other hand, the ζ-potential of the cationic poly(TMAEMA) brush layer had a large positive value (64.9 mV) and that of the anionic poly(SPMA) brush layer had a large negative value (−74.0 mV). The ζ-potential of the hydrophobic poly(BMA) brush layer was negative (−37.2 mV), which is typically observed at hydrophobic surfaces such as polyethylene, polytetrafluoroethylene, and poly(methyl methacrylate)[36,37] and caused by adsorbed electrolyte ions. From these results, the surface potential was successfully controlled by the chemical structure of the monomer unit. In particular, on the poly(TMAEMA), poly(SPMA), and poly(BMA) brush surfaces, forces derived from electrostatic interactions are expected, and on the poly(MPC) and poly(HEMA) brush surfaces, electrostatic forces are considered to be negligible. Although we must keep in mind that these results are obtained in a 10 mmol/L sodium chloride solution, it will, nevertheless, be easier to discuss electrostatic interaction on these surfaces.

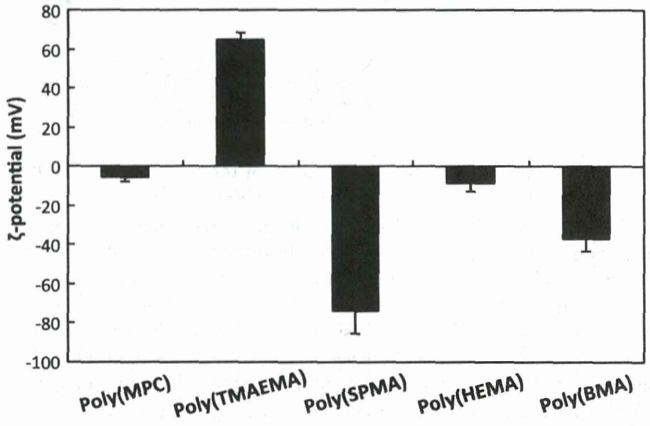

Figure 4. ζ-Potential of polymer brush surfaces in 10 mmol/L NaCl aqueous solution.

3.2. Interaction Force with Functional Groups on Polymer Brush Surfaces. The interaction force with different functional groups was evaluated by the *f*−*d* curve measurement with AFM.

Figure 5 shows the interaction force measured using a cantilever modified by a COOH−SAM, NH_2−SAM, or CH_3−SAM against each polymer brush surface. The zwitterionic poly(MPC) and the hydrophilic poly(HEMA) brush surfaces hardly interacted with any functional group, which corroborates the results that these surfaces are hydrophilic and electrically neutral. The cationic poly(TMAEMA) brush surface interacted strongly with the COOH−SAM surface. This is considered an electrostatic interaction between the positive charge of poly(TMAEMA) and the negative charge of the carboxyl group. In the case of the hydrophobic poly(BMA) brush surface, strong interaction forces were observed with CH_3−SAM, which is considered a hydrophobic interaction operating between hydrophobic surfaces. The hydrophobic poly(BMA) also interacted with the NH_2−SAM, which is considered an electrostatic interaction, because the poly(BMA) brush surface

dx.doi.org/10.1021/la404981k | *Langmuir* XXXX, XXX, XXX−XXX

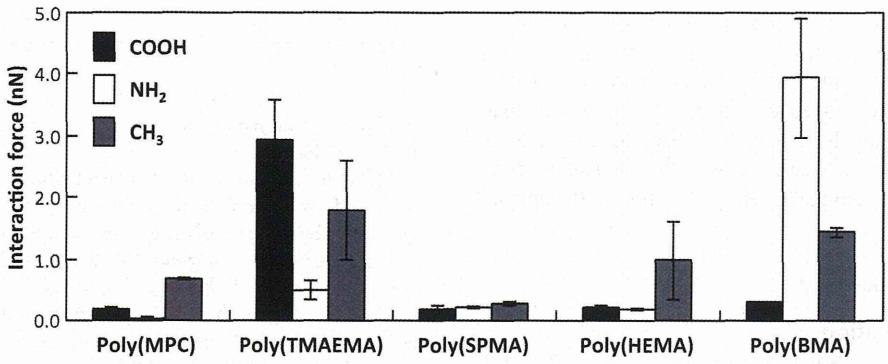

Figure 5. Interaction force between functional groups and polymer brush surfaces.

was negatively charged, as shown in the ζ-potential measurement. Contrary to expectation, the interaction force between the NH_2–SAM and the poly(SPMA) brush surface, which showed a large and negative ζ-potential in a 10 mmol/L sodium chloride solution, was very low in PBS. This resulted from an electrostatic shield, because a very strong interaction force between the NH_2–SAM and the poly(SPMA) brush surface was otherwise observed in pure water (data not shown).

3.3. Adsorbed Amount of Proteins on Polymer Brush Surfaces. The amount of proteins adsorbed on the polymer brush surfaces was quantified by SPR using Alb and Lys. The value of p*I* of Alb and Lys are 4.8 and 11.1, respectively, and they have respective net negative and net positive charges at pH 7.4. Therefore, we can investigate the effect of charge on protein adsorption using these two proteins.

Figure 6 shows the adsorbed amount of proteins on each polymer brush surface. Both the proteins were hardly adsorbed

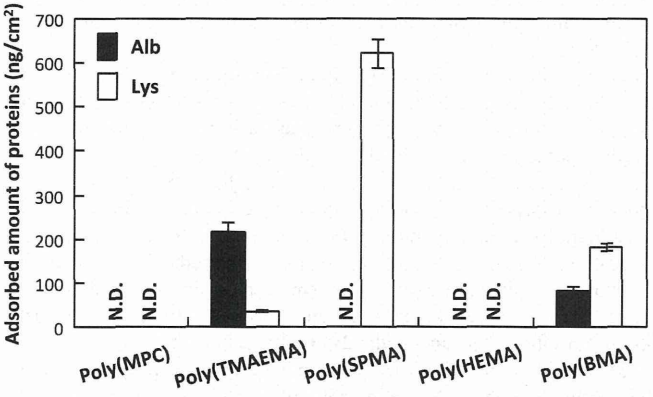

Figure 6. Adsorbed amount of proteins on the polymer brush surfaces.

on the zwitterionic poly(MPC) and hydrophilic poly(HEMA) brush surfaces. On the other hand, in the case of cationic poly(TMAEMA), anionic poly(SPMA), and hydrophobic poly(BMA) brush surfaces, ~100–700 ng/cm^2 of proteins adsorbed. In particular, on the cationic poly(TMAEMA) brush surface, the adsorbed amount of Alb was much higher than that of Lys; in contrast, on the anionic poly(SPMA) brush surface, an extremely large amount of Lys adsorbed, whereas Alb hardly adsorbed, which indicated the influence of charge at these surfaces. The adsorbed amount of Lys on the poly(BMA) brush surfaces was ~180 ng/cm^2, which is almost comparable to the theoretically calculated value of Lys monolayer adsorption (~170 ng/cm^2). From these results, the amount of adsorbed proteins depended on the physicochemical properties of surfaces and charge of proteins.

Here, we discuss the relationship between protein adsorption and interaction force by functional group. Although we must keep in mind that probes are forcibly moved toward the surface in the *f*–*d* curve measurement of AFM, the measurement in this study is considered to simulate the very early stage of protein adsorption in which proteins repeatedly approach and depart from the surface reversibly.

On the poly(MPC) and poly(HEMA) brush surfaces, which showed the lowest interaction forces with the functional groups, the adsorbed amount of proteins was extremely low with respect to both Alb and Lys. On the other hand, on the poly(TMAEMA) brush surface, which showed a strong interaction force with COOH–SAM, a large amount of protein with net negative charge adsorbed, which the adsorbed amount of protein with net positive charge was low. Moreover, on the poly(BMA) brush surface, which showed a strong interaction force with NH_2–SAM, the adsorbed amount of protein with net positive charge was higher than that of protein with a net negative charge. On the poly(MPC) and poly(HEMA) brush surfaces, which hardly interacted with any functional groups, it is proposed that proteins easily depart from the surfaces, leading to dramatic suppression of protein adsorption. In the case of the poly(TMAEMA) and poly(BMA) brush surface, which strongly interacted with functional groups, the detachment of the protein from the surfaces was difficult, which led to the large amount of protein being adsorbed. In the case of the poly(SPMA) brush surface, although the interaction forces were low even with NH_2–SAM in PBS, an extremely large amount of Lys still adsorbed. Therefore, the protein adsorption behavior on this surface is most likely dominated by interaction forces operating at different stages of the protein adsorption process. Investigation into the interaction forces operating on the polymer brush surface from different perspectives is currently under progress.

In summary, the methodology to quantitatively evaluate the nanoscale interaction forces at well-defined surfaces has been established by applying an AFM-based technique. Although more detailed research is necessary, interaction forces at the functional group level provide a good indication regarding protein adsorption.

4. CONCLUSIONS

We prepared five types of polymer brush layers with various physicochemical properties such as hydrophilicity and surface ζ-potential, which were controlled by the chemical structure of the monomer unit. The adsorbed amount of proteins depended

dx.doi.org/10.1021/la404981k | *Langmuir* XXXX, XXX, XXX–XXX

on the physicochemical properties of the polymer brush surfaces and the charge of the proteins. Moreover, various interaction forces were quantitatively evaluated with AFM using a functional-group-functionalized cantilever. We conclude that the direct measurement of the interaction force operating on a well-defined polymer brush surface will be a useful new analytical method for understanding protein adsorption behavior.

■ ASSOCIATED CONTENT

Supporting Information

XPS spectra of the polymer brush layers in the C_{1s}, N_{1s}, P_{2p}, and S_{2p} regions (Figure S1), height images of the polymer brush surfaces obtained by AFM under dry conditions (Figure S2), and relationship between the molecular weight of the polymer chains and the ellipsometric thickness of the polymer brush layers (Figure S3). This material is available free of charge via the Internet at http://pubs.acs.org.

■ AUTHOR INFORMATION

Corresponding Author

*E-mail: ishihara@mpc.t.u-tokyo.ac.jp. Tel: +81-3-5841-7124. Fax: +81-3-5841-8647.

Notes

The authors declare no competing financial interest.

■ ACKNOWLEDGMENTS

This work was supported by a Grant-in-Aid for Young Scientists (B) (Grant 24700475) from the Ministry of Education, Culture, Sports, Science and Technology (MEXT) of Japan and by a Health and Labour Sciences Research Grant (Grant H24-018) from the Ministry of Health, Labour, and Welfare of Japan.

■ REFERENCES

(1) Chen, H.; Yuan, L.; Song, W.; Wu, Z.; Li, D. Biocompatible polymer materials: Role of protein-surface interactions. *Prog. Polym. Sci.* **2008**, *33*, 1059−1087.

(2) *Proteins at Interfaces III, State of the art*; Horbett, T., Brash, J. L., Norde, W., Eds.; ACS Symposium Series 1120; American Chemical Society: Washington, DC, 2012.

(3) Leckband, D.; Israelachvili, J. Intermolecular forces in biology. *Q. Rev. Biophys.* **2001**, *34*, 105−267.

(4) Butt, H.-J.; Cappella, B.; Kappl, M. Force measurements with the atomic force microscope: Technique, interpretation and applications. *Surf. Sci. Rep.* **2005**, *59*, 1−152.

(5) Idiris, A.; Kidoaki, S.; Usui, K.; Maki, T.; Suzuki, H.; Ito, M.; Aoki, M.; Hayashizaki, Y.; Matsuda, T. Force measurement for antigen-antibody interaction by atomic force microscopy using a photograft-polymer spacer. *Biomacromolecules* **2005**, *6*, 2776−2784.

(6) Kienberger, F.; Kada, G.; Mueller, H.; Hinterdorfer, P. Single molecule studies of antibody-antigen interaction strength *versus* intramolecular antigen stability. *J. Mol. Biol.* **2005**, *347*, 597−606.

(7) Moore, N. W.; Mulder, D. J.; Kuhl, T. L. Adhesion from tethered ligand-receptors bonds with microsecond lifetimes. *Langmuir* **2008**, *24*, 1212−1218.

(8) Hanley, W.; McCarty, O.; Jadhav, S.; Tseng, Y.; Wirtz, D.; Konstantopoulos, K. Single molecule characterization of P-selectin/ligand binding. *J. Biol. Chem.* **2003**, *278*, 10556−10561.

(9) Kidoaki, S.; Matsuda, T. Adhesion forces of the blood plasma proteins on self-assembled monolayer surfaces of alkanethiolates with different functional groups measured by an atomic force microscope. *Langmuir* **1999**, *15*, 7639−7646.

(10) Sethuraman, A.; Han, M.; Kane, R. S.; Belfort, G. Effect of surface wettability on the adhesion of proteins. *Langmuir* **2004**, *20*, 7779−7788.

(11) Cho, E. C.; Kong, H.; Oh, T. B.; Cho, K. Protein adhesion regulated by the nanoscale surface conformation. *Soft Matter* **2012**, *8*, 11801−11808.

(12) Wei, Y.; Latour, R. A. Correlation between desorption force measured by atomic force microscopy and adsorption free energy measured by surface plasmon resonance spectroscopy for peptide-surface interactions. *Langmuir* **2010**, *26*, 18852−18861.

(13) Kidoaki, S.; Nakayama, Y.; Matsuda, T. Measurement of the interaction forces between proteins and iniferter-based graft-polymerized surfaces with an atomic froce microscope in aqueous media. *Langmuir* **2001**, *17*, 1080−1087.

(14) Inoue, Y.; Nakanishi, T.; Ishihara, K. Adhesion force of proteins against hydrophilic polymer brush surfaces. *React. Funct. Polym.* **2011**, *71*, 350−355.

(15) Lu, D. R.; Lee, S. J.; Park, K. Calculation of solvation interaction energies for protein adsorption on polymer surfaces. *J. Biomater. Sci., Polym. Ed.* **1991**, *3*, 127−147.

(16) Tsujii, Y.; Ohno, K.; Yamamoto, S.; Goto, A.; Fukuda, T. Structure and properties of high-density polymer brushes prepared by surface-initiated living radical polymerization. *Adv. Polym. Sci.* **2006**, *197*, 1−45.

(17) Inoue, Y.; Ishihara, K. Clarification of protein adsorption at polymer brush surfaces based on water structure surrounding the surface. In *Proteins at Interfaces III, State of the art*, Horbett, T., Brash, J. L., Norde, W., Eds.; ACS Symposium Series 1120; American Chemical Society: Washington, DC, 2012; pp 605−620.

(18) Iwata, R.; Suk-In, P.; Hoven, V. P.; Takahara, A.; Akiyoshi, K.; Iwasaki, Y. Control of nanobiointerfaces generated from well-defined biomimetic polymer brushes for protein and cell manipulations. *Biomacromolecules* **2004**, *5*, 2308−2314.

(19) Feng, W.; Brash, J. L.; Zhu, S. Non-biofouling materials prepared by atom transfer radical polymerization grafting of 2-methacryloyloxyethyl phosphorylcholine: Separate effects of graft density and chain length on protein repulsion. *Biomaterials* **2006**, *27*, 847−855.

(20) Yang, W.; Chen, S.; Cheng, G.; Vaisocherová, H.; Xue, H.; Li, W.; Zhang, J.; Jiang, S. Film thickness dependence of protein adsorption from blood serum and plasma onto poly(sulfobetaine)-grafted surfaces. *Langmuir* **2008**, *24*, 9211−9214.

(21) Yang, W.; Xue, H.; Li, W.; Zhang, J.; Jiang, S. Pursuing "zero" protein adsorption of poly(carboxybetaine) from undiluted blood serum and plasma. *Langmuir* **2009**, *25*, 11911−11916.

(22) Yoshikawa, C.; Goto, A.; Tsujii, Y.; Fukuda, T.; Kimura, T.; Yamamoto, K.; Kishida, A. Protein repellency of well-defined, concentrated poly(2-hydroxyethyl methacrylate) brushes by the size-exclusion effect. *Macromolecules* **2006**, *39*, 2284−2290.

(23) Wu, Z.; Chen, H.; Liu, X.; Zhang, Y.; Li, D.; Huang, H. Protein adsorption on poly(*N*-vinylpyrrolidone)-modified silicon surfaces prepared by surface-initiated atom transfer radical polymerization. *Langmuir* **2009**, *25*, 2900−2906.

(24) Gunkel, G.; Weinhart, M.; Becherer, T.; Haag, R.; Huck, W. T. S. Effect of polymer brush architecture on antibiofouling properties. *Biomacromolecules* **2011**, *12*, 4169−4172.

(25) Kitano, H.; Liu, Y.; Tokuwa, K.; Li, L.; Iwanaga, S.; Nakamura, M.; Kanayama, N.; Ohno, K.; Saruwatari, Y. Polymer brush with pendent glucosylurea groups constructed on a glass substrate by RAFT polymerization. *Eur. Polym. J.* **2012**, *48*, 1875−1882.

(26) Ishihara, K.; Ueda, T.; Nakabayashi, N. Preparation of phospholipid polymers and their properties as polymer hydrogel membranes. *Polym. J.* **1990**, *22*, 355−360.

(27) Inoue, Y.; Ishihara, K. Reduction of protein adsorption on well-characterized polymer brush layers with varying chemical structures. *Colloids Surf., B* **2010**, *81*, 350−357.

(28) Matyjaszewski, K.; Miller, P. J.; Shukla, N.; Immaraporn, B.; Gelman, A.; Luokala, B. B.; Siclovan, T. M.; Kickelbick, G.; Vallant, T.; Hoffmann, H.; Pakula, T. Polymers at interfaces: Using atom transfer

radical polymerization in the controlled growth of homopolymers and block copolymers from silicon surfaces in the absence of untethered sacrificial initiator. *Macromolecules* **1999**, *32*, 8716−8724.
(29) Husseman, M.; Malmström, E. E.; McNamara, M.; Mate, M.; Mecerreyes, D.; Benoit, D. G.; Hedrick, J. L.; Mansky, P.; Huang, E.; Russell, T. P.; Hawker, C. J. Controlled synthesis of polymer brushes by "living" free radical polymerization techniques. *Macromolecules* **1999**, *32*, 1424−1431.
(30) Yamamoto, K.; Miwa, Y.; Tanaka, H.; Sakaguchi, M.; Shimada, S. Living radical graft polymerization of methyl methacrylate to polyethylene film with typical and reverse atom transfer radical polymerization. *J. Polym. Sci., Part A: Polym. Chem.* **2002**, *40*, 3350−3359.
(31) Raiteri, R.; Preuss, M.; Grattarola, M.; Butt, H.-J. Preliminary results on the electrostatic double-layer force between two surfaces with high surface potentials. *Colloids Surf., A* **1998**, *136*, 191−197.
(32) Green, R. J.; Frazier, R. A.; Shakesheff, K. M.; Davies, M. C.; Roberts, C. J.; Tendler, S. J. B. Surface plasmon resonance analysis of dynamic biological interactions with biomaterials. *Biomaterials* **2000**, *21*, 1823−1835.
(33) Jones, D. M.; Brown, A. A.; Huck, W. T. S. Surface-initiated polymerizations in aqueous media: Effect of initiator density. *Langmuir* **2002**, *18*, 1265−1269.
(34) Hirata, I.; Morimoto, Y.; Murakami, Y.; Iwata, H.; Kitano, E.; Kitamura, H.; Ikada, Y. Study of complement activation on well-defined surfaces using surface plasmon resonance. *Colloids Surf., B* **2000**, *18*, 285−292.
(35) Currie, E. P. K.; Norde, W.; Stuart, M. A. C. Tethered polymer chains: Surface chemistry and their impact on colloidal and surface properties. *Adv. Colloid Interface Sci.* **2003**, *100−102*, 205−265.
(36) Hozumi, A.; Sugimura, H.; Yokogawa, Y.; Kameyama, T.; Takai, O. ζ-Potentials of planar silicon plates covered with alkyl- and fluoroalkylsilane self-assembled monolayers. *Colloids Surf., A* **2001**, *182*, 257−261.
(37) Yoshinari, M.; Kato, T.; Matsuzaka, K.; Hayakawa, T.; Inoue, T.; Oda, Y.; Okuda, K.; Shimono, M. Adsorption behavior of antimicrobial peptide Histatin 5 on PMMA. *J. Biomed. Mater. Res., Part B* **2006**, *77B*, 47−54.

dx.doi.org/10.1021/la404981k | *Langmuir* XXXX, XXX, XXX−XXX

OPEN ACCESS Freely available online

PLOS ONE

In Vitro Evaluation of the Risk of Inducing Bacterial Resistance to Disinfection Treatment with Photolysis of Hydrogen Peroxide

Hiroyo Ikai, Yu Odashima, Taro Kanno, Keisuke Nakamura, Midori Shirato, Keiichi Sasaki, Yoshimi Niwano*

Tohoku University Graduate School of Dentistry, Aoba-ku, Sendai, Japan

Abstract

The purpose of the present study was to evaluate the risk of inducing bacterial resistance to disinfection treatment with photolysis of H_2O_2 and comparing this with existing antibacterial agents. We tested seven antibacterial agents, including amoxicillin, cefepime hydrochloride, erythromycin, ofloxacin, clindamycin hydrochloride, ciprofloxacin hydrochloride, and minocycline hydrochloride, as positive controls for validation of the assay protocol. For all of the agents tested, at least one of the four bacterial species (*Staphylococcus aureus*, *Enterococcus faecalis*, *Escherichia coli*, and *Streptococcus salivarius*) was resistant to these agents by repeated exposure to subinhibitory concentrations of the agents up to 10 times. In contrast, antibacterial activity against any of the bacterial species tested (*S. aureus*, *E. faecalis*, *E. coli*, *S. salivarius*, *Pseudomonas aeruginosa*, *Streptococcus mutans*, and *Aggregatibacter actinomycetemcomitans*) was not affected by repeated exposure to the disinfection treatment up to 40 times. This finding suggested that the risk of inducing bacterial resistance by disinfection treatment was low. The active ingredient of this disinfection treatment is hydroxyl radicals generated by photolysis of H_2O_2. Therefore, hydroxyl radicals interact with several cell structures and different metabolic pathways in microbial cells, probably resulting in a lack of development of bacterial resistance. In conclusion, disinfection treatment with photolysis of H_2O_2 appears to be a potential alternative for existing antimicrobial agents in terms of a low risk of inducing bacterial resistance.

Citation: Ikai H, Odashima Y, Kanno T, Nakamura K, Shirato M, et al. (2013) *In Vitro* Evaluation of the Risk of Inducing Bacterial Resistance to Disinfection Treatment with Photolysis of Hydrogen Peroxide. PLoS ONE 8(11): e81316. doi:10.1371/journal.pone.0081316

Editor: Marie-Joelle Virolle, University Paris South, France

Received September 4, 2013; **Accepted** October 19, 2013; **Published** November 25, 2013

Funding: This research was supported by Ministry of Education, Science, Sports and Culture, Japan, Grant-in-Aid for Scientific Research (C), 23590144, 2011. The funder had no role in study design, data collection and analysis, decision to publish, or preparation of the manuscript.

Competing Interests: The authors have declared that no competing interests exist.

* E-mail: *niwano@m.tohoku.ac.jp

Introduction

Disinfection treatment, in which hydroxyl radicals generated by photolysis of hydrogen peroxide (H_2O_2) kill bacteria efficiently, has been developed in our laboratory [1,2]. *In vitro* studies found that *Staphylococcus aureus*, *Streptococcus mutans*, *Enterococcus faecalis*, and *Aggregatibacter actinomycetemcomitans* were killed with a >5-log reduction of viable counts within 3 min when bacterial suspension in 1 M H_2O_2 was irradiated with laser light at 405 nm [1]. One molar H_2O_2 corresponds to approximately 3%, which is a concentration used as a disinfectant for skin and oral mucosa. A subcommittee of the US Food and Drug Administration also concluded that H_2O_2 is safe at concentrations of up to 3% [3]. In addition to *in vitro* findings, an *in vivo* antibacterial effect of this disinfection system was proven effective in a rat model of superficial *S. aureus* infection [4].

Antibiotic-resistant bacteria are continuously emerging because of the widespread and sometimes indiscriminate use of antibiotics in the medical field [5,6]. Reactive oxygen species (ROS), such as hydroxyl radicals and singlet oxygen, non-specifically oxidize several cell structures, leading to cell death [7–9]. Consequently, it is unlikely that bacteria would develop resistance to the cytotoxic action of ROS [7–10]. Therefore, disinfection treatment using photolysis of H_2O_2 is not expected to induce bacterial resistance to this treatment either.

To assess the risk of developing bacterial resistance to antibiotics and antiseptics, monitoring minimal inhibitory concentrations (MICs) of these agents after serial passage of culture through subinhibitory concentrations of these agents has proven effective [11–13]. Therefore, in the present study, clinically available antibacterial agents were used as positive controls to validate the assay protocol. This was performed by evaluating if the test bacterial strains used in the present study would develop resistance to the agents by repeated exposure to subinhibitory concentrations of the agents.

The purpose of the present study was to determine if the risk of developing bacteria resistant to disinfection treatment using photolysis of H_2O_2 is low through repeated exposure of bacteria under the sublethal conditions in which the bacteria were not completely killed.

Materials and Methods

Bacteria

S. aureus JCM 2413, *E. faecalis* JCM 7783, *Escherichia coli* JCM 5491, *Streptococcus salivarius* JCM 5707, *Pseudomonas aeruginosa* JCM

6119, *S. mutans* JCM 5705, and *A. actinomycetemcomitans* JCM 2434, purchased from the Japan Collection of Microorganisms, RIKEN BioResource Center (Wako, Japan), were used. Suspensions of facultative anaerobic bacteria were prepared from cultures grown on brain heart infusion (BHI) agar (Becton Dickinson Labware, Franklin Lakes, NJ, USA) for *S. aureus*, *E. faecalis*, *E. coli*, and *S. salivarius*, and on desoxycholate-hydrogen sulfide-lactose (DHL) agar (Nissui, Tokyo, Japan) for *P. aeruginosa* aerobically at 37°C for 20 h. Suspensions of *S. mutans* and *A. actinomycetemcomitans* were from cultures grown anaerobically on BHI agar using the Anaero Pack (Mitsubishi Gas Chemical Company, Tokyo, Japan) at 37°C for 44 h. The viable count of each bacterial suspension in each antibacterial assay was adjusted to a given density as described in the following sections using a colorimeter (WPA CO7500 colorimeter, Biochrom, Cambridge, UK).

Susceptibility testing for antibacterial agents and repeated exposure of bacteria to the agents.

Microdilution plates in which antibacterial agents were dehydrated were custom fabricated by Eiken Chemical Co., Ltd. (Dry Plate Eiken, Tokyo, Japan) for a broth microdilution method to determine MICs as described by the Clinical and Laboratory Standards Institute M7-A7 [14]. The following seven antibacterial agents provided by Eiken Chemical Co., Ltd. were tested: a β-lactam antibiotic, amoxicillin (AMX), a cephem antibiotic, cefepime hydrochloride (CFPM), a macrolide antibiotic, erythromycin (EM), a fluoroquinolone antibiotic, ofloxacin (OFLX), a lincosamide antibiotic, clindamycin hydrochloride (CLDM), a fluoroquinolone antibiotic, ciprofloxacin hydrochloride (CPFX), and a tetracycline antibiotic, minocycline hydrochloride (MINO). Figure 1a shows a schematic illustration of the assay method. In brief, each bacterial species (*S. aureus*, *E. faecalis*, *E. coli*, and *S. salivarius*) grown on BHI agar was harvested and suspended in Muller-Hinton broth (Kanto Chemical Co., Inc., Tokyo, Japan). The number of colony-forming units (CFU) of each strain was adjusted to 1×10^5 CFU/mL. An aliquot (100 μL) of the resultant suspension was inoculated into a well of the plates. After incubation with a lid at 37°C for 20 h, bacterial growth was visually assessed to determine the MIC using a microplate reading mirror (Eiken Chemical Co., Ltd.). After determining the initial MICs, 20 μL of a bacterial suspension of a well showing 1/2 MIC was mixed with 1980 μL of Muller-Hinton broth to eliminate the effect of drug carry-over. A volume of 20 μL of the resultant suspension was then inoculated onto BHI agar followed by incubation at 37°C for 20 h. Bacterial suspensions were again prepared and MICs were determined as described above. The same procedure was repeatedly performed to assess the induction of bacterial resistance to the antibacterial agents tested (total number of treatments = 10). In the case of inconvenience for continuous working, a mixture of 20 μL of a bacterial suspension of a well showing 1/2 MIC and 1980 μL of Muller-Hinton broth was kept at 4°C until the next assay. An increase of four times or higher in MIC over the initial MIC was set as the criterion for inducing resistance to each antibacterial agent [15]. All tests were performed in duplicate (two independent assays).

Susceptibility testing for disinfection treatment with photolysis of H_2O_2 and repeated exposure of bacteria to this treatment

Disinfection treatment with photolysis of H_2O_2 was performed according to our previous study [1]. A continuous-wave laser device (RV-1000; Ricoh Optical Industries, Hanamaki, Japan) was used to photolyze H_2O_2. Three percent (w/v) H_2O_2 was prepared by diluting 31% (w/v) H_2O_2 (Santoku Chemical Industries, Tokyo, Japan) with phosphate-buffered saline (PBS, pH 7.4). Bacterial suspensions were prepared in PBS following incubation on the corresponding agar plates as described above, and the initial inoculum size of every bacterial species was adjusted to a range of 5×10^6 to 1×10^8 CFU/mL. Figure 1b shows a schematic illustration of the assay method. In a microplate well, 10 μL of the bacterial suspension was mixed with 190 μL of 3% H_2O_2 followed by laser light irradiation at 405 nm for 10 to 120 s at an irradiance of 930 mW/cm^2. Laser light irradiation time was preliminarily determined to obtain an approximately 2-log reduction in viable cell count in each bacterial species. This irradiation time was 120 s for *E. faecalis* and *S. salivarius*, 90 s for *S. aureus* and *S. mutans*, 30 s for *E. coli* and *A. actinomycetemcomitans*, and 10 s for *P. aeruginosa*. We confirmed that exposure of 3% H_2O_2 alone (without laser irradiation) for the given time as described above did not exert any bactericidal effect on any of the bacterial species tested. After irradiation, 50 μL of the treated bacterial suspension was added to 50 μL of sterile catalase solution (5000 U/mL) to terminate the bactericidal effect of the remaining H_2O_2. A 10-fold serial dilution of the mixture was then prepared using PBS, and 10 μL of the diluted solution was plated on the corresponding agar plate. Agar plates were incubated as described above at 37°C for 20 h or longer to determine the number of CFU/mL. The colonies grown on the agar plates were again suspended in PBS with the inoculum size in the range of 5×10^6 to 1×10^8 CFU/mL. The same procedure was then repeatedly performed to assess the induction of bacterial resistance to the treatment (the total number of treatments = 40). All tests were performed in triplicate (three independent assays).

Electron spin resonance (ESR) analysis for hydroxyl radicals generated by photolysis of H_2O_2

To confirm that hydroxyl radicals were generated time-dependently by photolysis of H_2O_2, hydroxyl radicals were quantitatively analyzed by an ESR-spin trapping technique as described in our previous studies [1,16]. In brief, H_2O_2 was mixed with 5,5-dimethyl-1-pyrroline *N*-oxide (DMPO; Labotec, Tokyo, Japan), a spin trap agent, in a microplate well to reach final concentrations of 3% (w/v) for H_2O_2 and 300 mM for DMPO. The sample was then irradiated with a laser light for 0, 10, 20, and 30 s. After irradiation, the sample was transferred to a quartz cell for ESR spectrometry, and the ESR spectrum was recorded on an X-band ESR spectrometer (JES-FA-100; JEOL, Tokyo, Japan). The measurement conditions for ESR were as follows: field sweep, 331.41–341.41 mT; field modulation frequency, 100 kHz; field modulation width, 0.1 mT; amplitude, 80; sweep time, 2 min; time constant, 0.03 s; microwave frequency, 9.420 GHz; and microwave power, 4 mW. The compound 4-hydroxy-2,2,6,6-tetramethylpiperidine (20 μM; Sigma Aldrich, St. Louis, MO, USA) was used as a standard to calculate the concentration of DMPO-OH, a spin adduct of hydroxyl radicals. The concentration of DMPO-OH was determined using Digital Data Processing (JEOL). All assays were performed in triplicate (three independent assays).

Results

Susceptibility testing for antibacterial agents

Table 1 summarizes the MICs at the first, fifth, and tenth exposure of each bacterial species to antibacterial agents tested. The initial MICs of all the seven antibacterial agents against *S. aureus* were within a narrow range between 0.12 and 0.5 μg/mL, and the values become higher at the fifth and tenth exposure. Especially the MICs of CFPN and CLDM at the tenth exposure were 128 and 32 μg/mL, respectively. The initial MICs of the